Wireless Networks (2023) 29:2471–2480
https://doi.org/10.1007/s11276-023-03285-w

ORIGINAL PAPER

# Prediction of path loss in coastal and vegetative environments with deep learning at 5G sub-6 GHz

Kiyas Kayaalp[1] · Sedat Metlek[2] · Abdullah Genc[3] · Habib Dogan[4] · İbrahim Bahadir Basyigit[5]

Accepted: 15 February 2023 / Published online: 8 April 2023
© The Author(s), under exclusive licence to Springer Science+Business Media, LLC, part of Springer Nature 2023

## Abstract

Path loss prediction is quite important for the network performance of the wireless sensors, quality of cellular communication-based link budget, and optimization of coverage planning in mobile networks. With the development of 5G technology, even though different log-distance path loss models are generated for these, new-developed methods are required to make models more flexible and accurate for complex environments. In this study, for different coastal terrains (air-dry sand, wet sand, small pebble, big pebble) and various vegetable areas (pine, orange, cherry, and walnut), the principle and procedure of deep learning-based path loss prediction are provided in 3.5 GHz, 3.8 GHz, and 4.2 GHz in the 5G frequency zone, as a novelty. For this, recurrent neural network (RNN) and long short-term memory (LSTM) methods are proposed. The test sample number is 240 since 20% of all datasets (1200) are test data. In general, path loss for coastal terrains is higher than path loss for vegetation areas with an average of 5 dB. For both coastal terrains and vegetation areas, the recurrent neural network method predicts better than the long short-term memory method. Consequently, for both coastal terrains and vegetation areas, RNN models with $R^2$ values of 0.9677 and 0.9042, respectively, are preferred.

**Keywords** Path loss · 5G · Deep learning · LSTM · RNN · Coastal terrains · Vegetative environments

✉ İbrahim Bahadir Basyigit
bahadirbasyigit@isparta.edu.tr

Kiyas Kayaalp
kiyaskayaalp@siparta.edu.tr

Sedat Metlek
sedatmetlek@mehmetakif.edu.tr

Abdullah Genc
abdullahgenc@isparta.edu.tr

Habib Dogan
hdogan@mehmetakif.edu.tr

[1] Department of Computer Engineering, Isparta University of Applied Sciences, Isparta, Turkey

[2] Department of Electronics and Automation, Burdur Mehmet Akif Ersoy University, Burdur, Turkey

[3] Department of Mechatronics Engineering, Isparta University of Applied Sciences, Isparta, Turkey

[4] Department of Computer Technologies and Information Systems, Burdur Mehmet Akif Ersoy University, Burdur, Turkey

[5] Department of Computer Technology, Isparta University of Applied Sciences, Isparta, Turkey

## 1 Introduction

Radio wave propagation has a significant contribution not only to the research but also to the development process of wireless communication systems. The signal strength of these wireless network systems decreases with increasing distance between transmitter ($T_x$) and receiver ($R_x$) [1]. Radio wave propagation characteristics vary according to the environment due to electromagnetic (EM) effects such as scattering, reflection, or diffraction [2]. These effects cause a complex propagation environment and make it difficult to accurately calculate the received signal strength [3]. Therefore, there is a need for different prediction models specific to each external environment, with reference to measurement data.

As electromagnetic (EM) signals propagate into the environment, they attenuate at a certain distance. The decrease in signal power of the EM wave can be defined as path loss [4]. Accurate estimation of path loss plays an important role in the link budget of the mobile network, the estimation of cellular communication coverage, RF optimization affecting the system performance, and the

determination of the number and location of base stations [5]. These encourage engineers and researchers to generate accurate models at different frequencies according to the target audience in various outdoor/indoor environments [6–8]. In order to generate and evaluate these models, measurements are conducted in different scenarios, and data are collected.

Many experimentally obtained path loss models such as the log-normal model (LNM) and modified exponential decay (MED) model (Weissberger, ITU Recommendation (ITU- R), LITU-R, FITU-R, and COST235) are commonly used in the different forest [9, 10] and, vegetative [11, 12] areas or various terrains such as grassy [13], snowy [14], and sandy [15] environments to estimate path loss.

The main parameter that determines the RF propagation and channel properties of the electromagnetic wave in the indoor and outdoor environment is path loss [16]. Even though studies on radio wave propagation in forest environments are common [6, 17–20], pebble and sand environments are not studied extensively. In some cases, radio propagation is studied for tracking animal grazing in large terrains [21]. A sample of works utilizes the free-space path loss (FSPL) model [22], two-ray model [23], ray-tracing model [24], and knife-edge diffraction model [25] in various areas. However, these studies show that the effects on path loss are not similar, as each different environment has its own channel characteristics. Therefore, the lack of accurate models causes inadequate and incomplete results of using WSN in coverage planning. The wide variety of these propagation models allows WSNs to monitor and track targets accurately [26, 27]. Also, the research studies [28] point out that the propagation of RF has different effects on various terrains. Therefore, it becomes an important need to effectively determine the effects of terrain changes on path loss in various environments.

This study is made to overcome the problems mentioned above and to generate more accurate path loss models. The proposed models can be utilized not only for tracking bird feeding habits but also for monitoring sports activities and environmental/ground surveillance of the coastal pebble environments. Unlike path loss models, pebbles can also be tracked using active RFID [29, 30]. In addition to monitoring pebble mobility, the proposed model can also contribute to the recovery process in flood-type avalanches that may occur in Gravel-Bed Rivers. On the other hand, the proposed models are expected to support the coverage planning tools to obtain more accurate channel characterizations. Finally, proposed models, which are expected to be used in applications such as the Internet of Things, can be effective with WSN in controlling the pebbles laid on the ground at home and garden design and in monitoring rural areas using pebbles. In addition to these scenarios and also many other cases [31–33], anticipated applications of WSN and mobile network is constantly evolving and changing. This reveals the importance of accurate channel features. In coastal, forest, and vegetation areas, the measurement of most of the widely known path loss models is conducted in a temperate climate. However, these models may not be successful in tropical climates due to the high humidity effect. The amount of humidity is an important parameter that changes the dielectric constant and the propagation properties of the electromagnetic wave [12]. So, more attenuation is expected in tropical climates than in temperate climates.

There are several reasons why the measurements in this study were made in a 5G frequency region. Today's 5G networks are designed to increase the throughput data, expand the coverage area, develop the density of connection, decrease radio latency, and expand spectral efficiency. Wireless network, which supports the Internet of Things (IoT) applications, provides increased coverage of different terrains [34]. Furthermore, millimeter wave and sub-6 GHz bands are likely to be used as they provide wide bandwidths. In addition to collecting attenuation data by performing various measurements and drive tests for these new frequencies, verification of these measurement results in different environments is important for the correct estimation of the generated model [35]. Thus, the coverage area of the 5G mobile network is efficient and the number of stations is optimum.

There are several studies to predict path loss with deep learning methods [36, 37]. However, to the best of our knowledge, there is no study on the prediction of the coastal environment and the vegetative environment examined in this study by the deep learning method. In this paper, propagation models are generated for different coastal terrains and vegetation environments by means of the deep learning method. For 3.5 GHz, 3.8 GHz, and 4.2 GHz as in 5G regions (below 6 GHz) in order to break the uncertainty of path loss. While these coastal terrains are air-sand, wet-sand, small, and big pebble areas, vegetation environments consist of pine, orange, cherry, and walnut areas.

Section 2 covers the measurement environment and data acquisition. Section 3 provides the design of DNN models consisting of Recurrent Neural Network (RNN) and Long Short-Term Memory (LSTM). Section 4 includes the results and comparison. Section 5 gives the conclusion.

## 2 Measurement environment and data acquisition

Generally, the path loss model of the vegetation environments and coastal terrains can be identified as Eqs. 1 and 2.

$$PL_{vegetation}[dB] = a.f^{b}.d^{c} \quad (1)$$

$$PL(d)_{log-normal}[dB] = PL(d_0) + 10nlog_{10}(\frac{d}{d_0}) \quad (2)$$

Here, for Eq. 1, *a, b*, and *c* parameters are constants. In Eq. 2, for the model of first-order log-normal is PL (*d*) in dB, obstacles and various terrain effects are also taken into account. *d* is the distance between the $T_x$ and $R_x$ in meters, $d_0$ is the reference distance in meters, and *f* is the operating frequency in GHz.

The measurement environment in various coastal terrains and vegetation areas is given in Fig. 1. Accordingly, coastal terrains consist of small pebbles, big pebbles, air-dry sand, and wet sand. Also, vegetation areas cover pine, orange, cherry, and walnut trees. Measurement set-up consists of a vector signal generator operating in 50 MHz-6 GHz and Minicircuit RF pre-amplifier (ZVA-183X-S + model) with 26 dB gain ad 700 MHz-18 GHz operated range, two double ridged horn antennas (A-info LB-10180) with 1–18 GHz, a spectrum analyzer (Signal Hound USBSA44B) operating in the range of 1 Hz-4.4 GHz. The specifications of measurement are also given in Table 1. The signals are captured by the Spectrum Analyzer (Signal Hound USB-SA44B model operating in the range of 1 Hz-4.4 GHz) having Spike spectrum analyzer software with 30 kHz of bandwidth and stored into a control computer in order to be processed with codes in MATLAB® software. While the $T_x$ tripod is held still throughout the measurement, the $R_x$ tripod moves continuously throughout the main loop of $R_x$. Since the measurement interval is 1 m and $R_x$ levels are recorded for 5 s at each measurement point. The loss of RF cables is 5.6 dB. In the measurement data, system calibration is done by removing cable losses and antenna gain.

**Table 1** The parameters of the measurement setup

| Parameters | Description |
|---|---|
| Software for measurement | Spike spectrum analyzer |
| Transmit power | + 50 dBm |
| Transmit frequency | 3.5, 3.8, and 4.2 GHz |
| Transmit signal | Sinusoid |
| Antenna type (for both Tx and Rx) | Double-ridged horn antenna |
| Antenna gain | 12 dBi |
| Antenna polarization | Vertical |
| Antenna radiation pattern | Directional |
| Receiver antenna height | 2 m |
| Transmitter antenna height | 2 m |
| Bandwidth | 30 kHz |
| Signal generator | 50 MHz–6 GHz |

## 3 The design of DNN models

Nowadays, artificial intelligence methods are used in various applications such as classification and curve fitting. Since the datasets used in this study, which are regression data, include auto-correlation, recurrent neural network (RNN), and long short-term memory (LSTM) methods are preferred [38–42].

Two different datasets are created in the study. The first dataset consists of 1,200 data obtained from various grounds covered by small pebbles, big pebbles, air-dry sand, and wet sand. The second data set consists of 1,200 data obtained from various environments with pine, orange, cherry, and walnut trees. The algorithms used are developed in the MATLAB® environment, and the training and testing processes are carried out on a computer with an Intel Core i7-4702MQ@2.2 GHz processor and 16 GB RAM.

The flowchart with data acquisition, modeling, and model evaluation is given in Fig. 2. The data obtained by

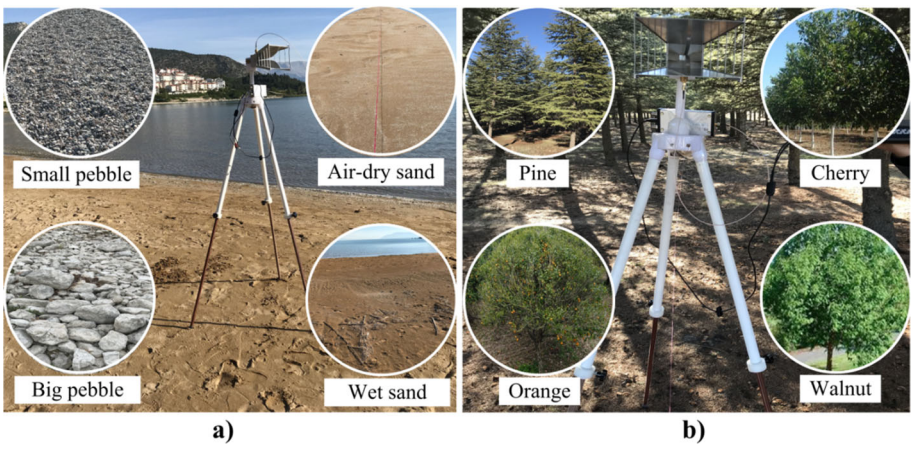


**Fig. 1** Measurement environment, four different **a** coastal terrains and **b** vegetation areas

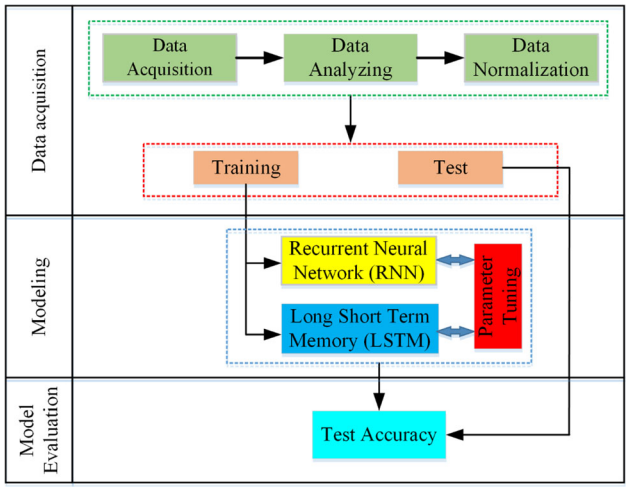


**Fig. 2** The flowchart with data acquisition, modeling, and model evaluation

the steps mentioned in Sect. 2 are normalized after analysis. They are divided into training and test according to the K-fold 5 value. During the training process, the model is trained until it reaches 0.001 error or 10,000 iterations. Then, it is trained with the hyper-parameter values specified in both algorithms separately.

Input and output parameters of the proposed DNN model are provided in Table 2. DNN models applied for both coastal terrains and vegetation areas have 3 inputs and 1 output. While the distance between $T_x$-$R_x$, frequency, and environment type shows the inputs, while the path loss value indicates the output. The distance, which is the first input, takes 100 different values since the measurement intervals are 1 m. For the second input, frequency takes three different values: 3.5 GHz, 3.8 GHz, and 4.2 GHz. The third input, which is environment type (coastal terrain/vegetation type), takes 4 different values. and the output value is PL varying between 20 and 100 dB. 1200 data is obtained by multiplying the numbers of different states of 3 inputs ($100 \times 4 \times 3$). For both environments, both LSTM and RNN methods are utilized to determine in which environment these methods are most successful. Thus, it is possible to break the uncertainty of path loss in the environment.

### 3.1 Recurrent neural network (RNN)

Recently, artificial neural network (ANN) models based on biological neural networks are utilized in many sectors from health to the military, especially because they can provide solutions to non-linear problems [43–45]. For this reason, new ANN models have been developed for many problems and one of these models is RNN [46]. In Figs. 3a and 3b, RNN and Feed Forward Neural Network (FFNN) structures with hidden layers and neurons in these layers are given. Even if RNN given in seem very similar to the FFNN structure in general, there are some fundamental differences [47]. The most significant difference is that the output of each cell in the model is taken as its input in the next iteration. Since the data used in this study are sequential, the RNN method is preferred. There are many variants of the RNN method in the literature [48].

The total output value of an RNN cell is given in Eq. 3. Here, the terms can be expressed that $x_t$ is the input value in tth step, $U$ is the weight coefficient of the input value, $f_{sum}$ is the output value of the cell in $(t-1)$th step, and $w$ is the weight of the output value, and $b$ is the bias values.

$$f_{sum} = (x_t.U + f_{net-1}.w) + b \tag{3}$$

In Eq. 4, it is given that $f_{sum}$ value obtained from the cell is transferred to the activation function. $f_{net}$ value represents the cell's output at $t^{th}$ step. Various activation functions in the literature and their results are presented in detail in Fig. 4. Also, the formulas of the sigmoid, tanh, ReLU and softplus activation functions are shown in Eqs. (5–8), respectively.

$$f_{net} = Act_{fonk}(f_{sum}) \tag{4}$$

**Table 2** Input and output parameters of the proposed DNN model

| Environment | Inputs/output | Parameters | Range | # of different state |
|---|---|---|---|---|
| DNN models for various coastal terrains | Inputs | Distance, d | 0–100 m | 100 |
| | | Frequency, f | 3.5, 3.8, and 4.2 GHz | 3 |
| | Output | Coastal terrain type | Small/big pebble, air-dry/wet sand | 4 |
| | | Path loss, PL | 20–100 dB | – |
| DNN models for various vegetation areas | Inputs | Distance, d | 0–100 m | 100 |
| | | Frequency, f | 3.5, 3.8, and 4.2 GHz | 3 |
| | Output | Vegetation type | Pine, orange, cherry, and walnut trees | 4 |
| | | Path loss, PL | 20–100 dB | – |

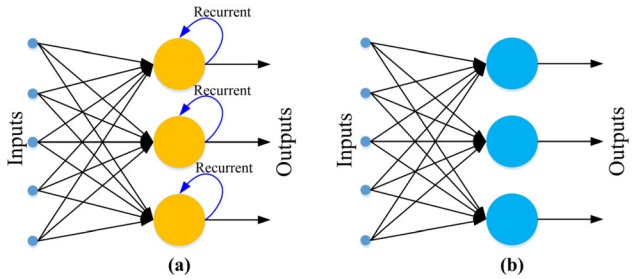


**Fig. 3** Recurrent Neural Network and Feed Forward Neural Network structures

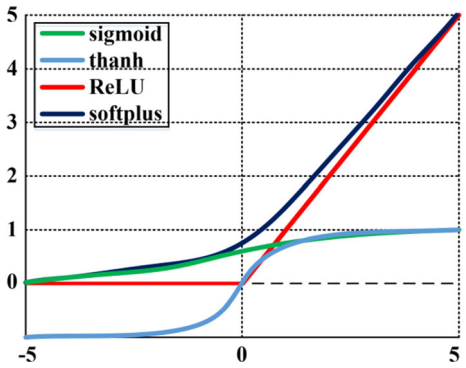


**Fig. 4** Various activation functions

$$f_{Net} = \frac{1}{1 + e^{-f_{sum}}} \, for \, \text{sigmoid} \tag{5}$$

$$f_{Net} = tanh(f_{sum}) \, for \, \tanh \tag{6}$$

$$f_{Net} = max(0, f_{sum}) \, for \, \text{ReLU} \tag{7}$$

$$f_{Net} = \ln\left(1 + e^{f_{sum}}\right) for \, \text{softplus} \tag{8}$$

### 3.2 Long Short-Term Memory (LSTM)

RNNs usually perform operations by keeping the value from the previous iteration in their memory. RNNs work accurately if the value in the last iteration is highly dependent on the value of the previous iteration. However, the success rate decreases if the last iteration value is related to the values before 5–10 iterations as shown in Fig. 5. The LSTM method has been developed to resolve this shortcoming [49].

In the LSTM model, the dependence of the current value on the previous value can be defined significantly. While a typical RNN cell consists of a single cell and parallel structures as shown in Fig. 3(a), in the LSTM structure, these cells are serially connected to each other as repeating modules. Another difference between LSTM from RNN is that while there is only one layer in the RNN cell, there are four different layers interacting with each other in the LSTM cell as shown in Fig. 6. The functions, that allow deciding which information in these layers to pass, how much, and how, act as a gate.

An LSTM module consists of four functions input gate (i), forget gate (f), cell candidate (g), and output gate (o) as shown in Eqs. (9–12).

$$i_t = \sigma(W_i x_t + R_i h_{t-1} + b_i) \tag{9}$$

$$f_t = \sigma\left(W_f x_t + R_f h_{t-1} + b_f\right) \tag{10}$$

$$g_t = tanh\left(W_g x_t + R_g h_{t-1} + b_g\right) \tag{11}$$

$$o_t = \sigma(W_o x_t + R_o h_{t-1} + b_o) \tag{12}$$

Here, $W$, $x$, $R$, and $b$ terms used in these equations are input weight, inputs, recursive weight, and bias, respectively. The term $\sigma$ expresses the sigmoid function in Eq. 13, and the term $h_t$ is given in Eq. 14. In addition, $\odot$ represents the Hadamard term.

$$\sigma(x) = (1 + e^{-x})^{-1} \tag{13}$$

$$h_t = o_t \odot tanh_{(ct)} \tag{14}$$

## 4 Results

Parameters used for the LSTM and RNN models are provided in Table 3. Data obtained from measurements are trained with the hyper-parameters specified in both algorithms separately. To determine the best performance of the models, the tested hyperparameters are determined at certain intervals using the gradient descent method. Accordingly, while the initial learning rate of LSTM varies

**Fig. 5** The structures of LSTM

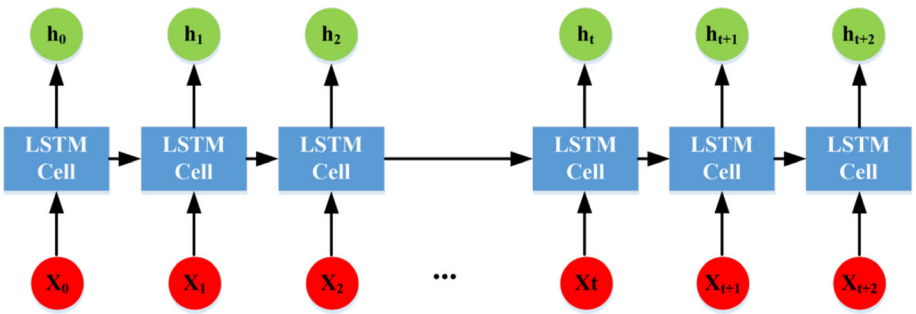

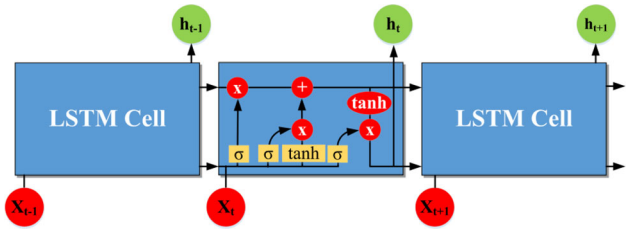


**Fig. 6** Four different layers within a repeating module in an LSTM

between 10−3–0, the number of neurons in the hidden layer of RNN range from 1 to 10.

In any soft-computing application, measuring the success of algorithms is as important as the preferred algorithm. For this, the error of the system is obtained by calculating the difference between the predicted and actual (measured) values in the developed systems. Therefore, some well-known metrics as the mean absolute error (MAE), root mean squared error (RMSE), and R-squared ($R^2$) are utilized to evaluate the success of the proposed methods [43]. A success criterion for the estimation of outputs of this study is shown in Table 4. For both coastal terrains and vegetation areas, RNN models with $R^2$ values of 0.9677 and 0.9042, respectively, are preferred. It should be noted that even though the LSTM method is generally more advanced and up-to-date than RNN, the RNN method is more successful due to the structure of the data set in this study.

A comparison of the predicted and measured results for both coastal terrains and vegetation areas are given in Table 5 with 5 different inputs. Accordingly, these inputs are randomly selected for each parameter. While PL values for coastal terrains are in the range of 23.38 dB to 84.74 dB, and PL values for vegetation areas vary between 26.05 dB to 86.32 dB. As seen in Table 5, RNN and LSTM values are quite close to each other.

A comparison of normalized values of RNN, LSTM, and measured results is depicted in Fig. 7 according to the test sample numbers. The test sample number is 240 since 20% of all datasets (1200) are test data. For both coastal

**Table 3** Parameters used for the LSTM and RNN model

| | Hyper-parameters | Tested hyper-parameters range | Best parameters for coastal terrains | Best parameters for vegetation areas |
|---|---|---|---|---|
| LSTM | Initial learning rate | $10^{-3}$–0 | $4 \times 10^{-3}$ | $7 \times 10^{-2}$ |
| | Dropout rate | 0.01–0.9 | 0.12 | 0.57 |
| | Batch size | 3–8 | 6 | 6 |
| | Learn rate drop period | 25–250 | 125 | 125 |
| | Learn rate drop factor | 0.01–0.8 | 0.25 | 0.35 |
| | Max epoch iterations | 100–10,000 | 745 | 980 |
| | Fully connected layer | 15–200 | 150 | 150 |
| | Dropout layer | 0.1–0.9 | 0.5 | 0.5 |
| RNN | Hidden layer number | 1–20 | 7 | 8 |
| | The number of neurons in the hidden layer | 1–10 | 10 | 7 |
| | Training functions | Levenberg–Marquardt (trainlm) | trainbr | trainbr |
| | | Bayesian Regularization (trainbr) | | |
| | Goal | 0.001–0.01 | 0.07 | 0.05 |
| | Max epoch iterations | 0–10,000 | 375 | 803 |

**Table 4** Success criteria for the estimation of outputs

| | DNN models | RMSE | MAE | $R^2$ |
|---|---|---|---|---|
| DNN Models for various coastal terrains | LSTM | 2.0751 | 1.5958 | 0.9631 |
| | RNN | 1.9670 | 1.2218 | 0.9677 |
| DNN Models for various vegetation areas | LSTM | 4.5678 | 3.5787 | 0.8981 |
| | RNN | 4.3624 | 3.2368 | 0.9042 |

**Table 5** Comparison of the predicted and measured results

| | Distance | Environment type | Frequency | Path loss | | |
|---|---|---|---|---|---|---|
| | | | | Measured | RNN | LSTM |
| Coastal terrains | 144 | Air-dry sand | 3.5 | 76.75 | 76.71 | 76.78 |
| | 140 | Big pebble | 3.8 | 82.39 | 82.37 | 82.45 |
| | 96 | Wet sand | 4.2 | 74.66 | 74.62 | 74.65 |
| | 148 | Small pebble | 3.8 | 76.78 | 76.72 | 76.74 |
| | 132 | Small pebble | 3.5 | 76.84 | 76.80 | 76.76 |
| Vegetation areas | 78 | Orange | 3.8 | 78.68 | 78.80 | 78.81 |
| | 56 | Walnut | 4.2 | 84.45 | 84.50 | 84.52 |
| | 48 | Orange | 3.5 | 73.04 | 73.04 | 73.04 |
| | 4 | Cherry | 4.2 | 26.05 | 26.05 | 26.05 |
| | 32 | Cherry | 4.2 | 74.11 | 74.11 | 74.11 |

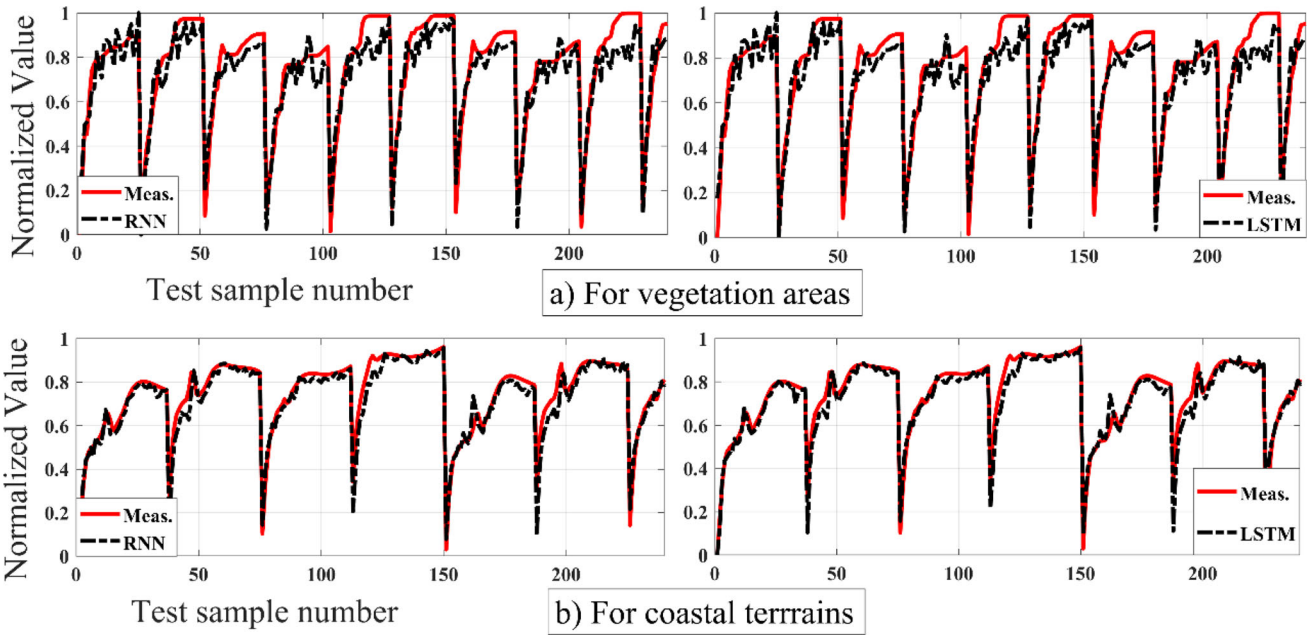


**Fig. 7** Comparison of normalized values of measured, RNN, and LSTM results for both vegetation areas and coastal terrains

terrains and vegetation areas, the RNN method predicts better than the LSTM method. It is noted that output results are predicted for four coastal terrains and for four vegetation areas at three different frequencies (3.5 GHz, 3.8 GHz, and 4.2 GHz). Instead of evaluating the path loss value for each frequency of these 8 environments, results can be drawn for 3.5 GHz of a randomly preferred environment. Therefore, wet-sand terrain from the coastal terrain group and cherry trees from the vegetation area group is selected and the variation of path loss values with respect to distance is given in Fig. 8. As can be seen, the RNN and LSTM results are consistent with the measured values. In addition, in both cases, the path loss increases rapidly up to about 10 m, while for further distances, it first increases slowly and then continues at a constant oscillation.

## 5 Conclusion

Accurate propagation modeling is of great importance to the accuracy of link budget, coverage planning, network performance, and optimization efficiency of mobile communication and wireless sensors. Accordingly, path loss prediction and radio channel modeling are widely studied by means of machine learning methods. In this study, for 8 different complex environments, four coastal terrains, and four vegetable areas, novel path loss models are developed

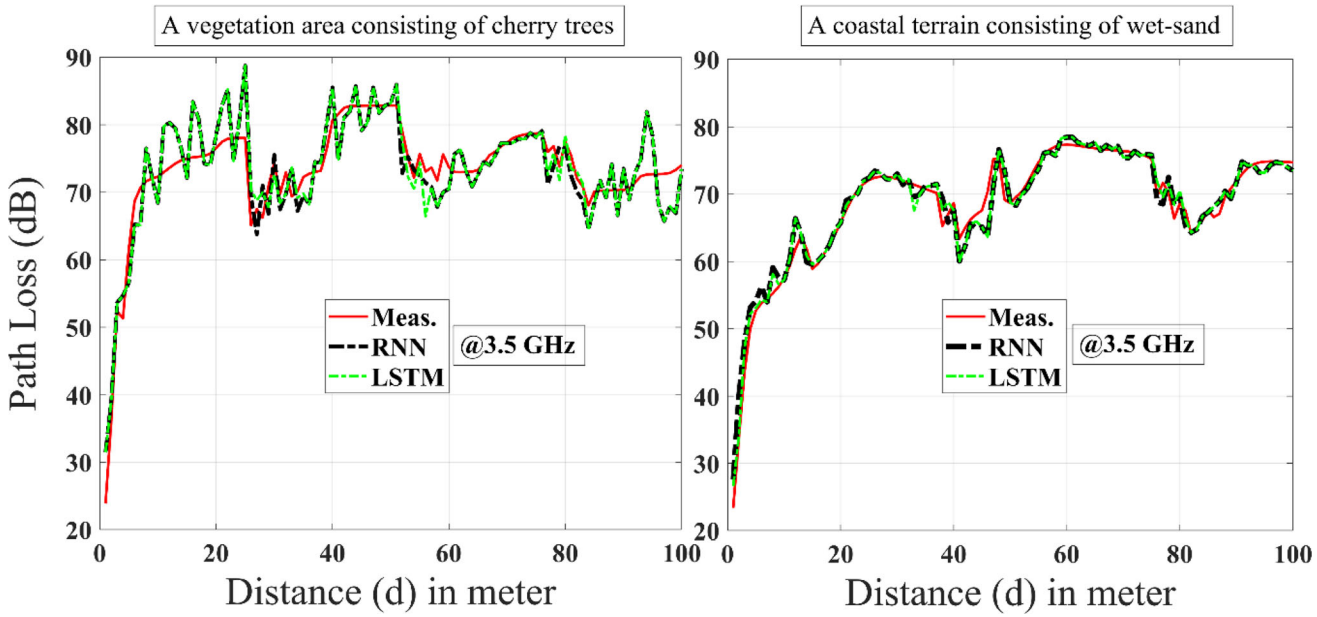


**Fig. 8** Comparison of PL values of measured, RNN, and LSTM results for both vegetation areas consisting of cherry trees and wet-sand terrains

with deep learning techniques: RNN and LSTM. While these coastal terrains are air-sand, wet-sand, small, and big pebble areas, vegetation environments consist of pine, orange, cherry, and walnut areas. Measurements are made at frequencies of 3.5 GHz, 3.8 GHz, and 4.2 GHz, which are known as sub-6 GHz and located within the 5G frequency region. Data from measurement results are divided into training and test according to the K-fold 5 value. During the training process, the model is trained until it reaches 0.001 error or 10,000 iterations. Then, it is trained with the hyper-parameter values specified in both algorithms separately. RMSE, MAE, and R2 values of both RNN and LSTM models are compared. For both coastal terrains and vegetation areas, key results show that models with RMSE values of 1.9670 and 4.3624, respectively, are preferred. It should be noted that even though the LSTM method is generally more advanced and up-to-date than RNN, the RNN method is more successful due to the structure of the data set in this paper. Examination of snowy and rainy (humid) weather conditions on the same lands on path loss is a future study.

## References


1. Cheerla, S., Ratnam, D. V., & Borra, H. S. (2018). Neural network-based path loss model for cellular mobile networks at 800 and 1800 MHz bands. *AEU-International Journal of Electronics and Communications, 94*, 179–186.
2. Hejselbaek, J., Odum Nielsen, J., Fan, W., & Pedersen, G. F. (2018). Empirical study of near ground propagation in forest terrain for internet-of-things type device-to-device communication. *IEEE Access*, *6*, 54052–54063.
3. Azevedo, J. A., & Santos, F. E. (2017). A model to estimate the path loss in areas with foliage of trees. *AEU-International Journal of Electronics and Communications, 71*, 157–161.
4. Eras, L. E. C., Silva, D. K. N. D., Barros, F. B., Correia, L. M., & Cavalcante, G. P. S. (2018). A radio propagation model for mixed paths in amazon environments for the uhf band. *Wireless Communications and Mobile Computing, 2018*, 1–15.
5. Basyigit, I. B., & Dogan, H. (2020). Troubleshooting of handover problems in 900 MHz for speech quality. *Wireless Personal Communications, 114*, 1833–1845.
6. Picallo, I., Klaina, H., Lopez-Iturri, P., Aguirre, E., Celaya-Echarri, M., Azpilicueta, L., Eguizábal, A., Falcone, F., & Alejos, A. (2019). A radio channel model for d2d communications blocked by single trees in forest environments. *Sensors, 19*(21), 4606. https://doi.org/10.3390/s19214606.
7. Cama-Pinto, D., & Damas, A. (2019). Path loss determination using linear and cubic regression inside a classic tomato greenhouse. *International Journal of Environmental Research and Public Health, 16*(10), 1744.
8. Raheemah, A., Sabri, N., Salim, M. S., Ehkan, P., & Ahmad, R. B. (2016). New empirical path loss model for wireless sensor networks in mango greenhouses. *Computers and Electronics in Agriculture, 127*, 553–560.
9. Genc, A. (2021). A new path loss model based on the volumetric occupancy rate for the pine forests at 5G frequency band. *International Journal of Microwave and Wireless Technologies, 13*(2), 144–153.
10. Meng, Y. S., & Lee, Y. H. (2009). Empirical near ground path loss modeling in a forest at VHF and UHF bands. *IEEE Transactions on Antennas and Propagation, 57*(5), 1461–1468.
11. Dogan, H. (2021). A new empirical propagation model depending on volumetric density in citrus orchards for wireless sensor network applications at sub-6 GHz frequency region. *International Journal of RF and Microwave Computer-Aided Engineering, e22778*, 1–10.
12. Rao, T. R., & Balachander, D. (2013). Ultra-high frequency near-ground short-range propagation measurements in forest and

plantation environments for wireless sensor networks. *IET Wireless Sensor Systems, 3*(1), 80–84.
13. Olasupo, T. O., & Otero, C. E. (2016). Empirical path loss models for wireless sensor network deployments in short and tall natural grass environments. *IEEE Transactions on Antennas and Propagation, 64*(9), 4012–4021.
14. Cheffena, M., & Mohamed, M. (2017). Empirical path loss models for wireless sensor network deployment in snowy environments. *IEEE Antennas and Wireless Propagation Letters, 16*, 2877–2880.
15. Alsayyari, A., & Kostanic, I. (2014) An empirical path loss model for wireless sensor network deployment in a sand terrain environment. In: *2014 IEEE World Forum on Internet of Things (WF-IoT)*, pp. 218–223.
16. Li, Q., & Zhang, H. (2019). A new method for path-loss modeling. *International Journal of Microwave and Wireless Technologies, 11*(8), 739–746.
17. Kurnaz, O., & Helhel, S. (2014). Near ground propagation model for pine tree forest environment. *AEU-International Journal of Electronics and Communications, 68*(10), 944–950.
18. Leonor, N. R., & Caldeirinha, R. F. (2014). A 2D ray-tracing based model for micro-and millimeter-wave propagation through vegetation. *IEEE Transactions on Antennas and Propagation, 62*(12), 6443–6453.
19. Gay-Fernández, J. A., & Cuinas, I. (2014). Short-term modeling in vegetation media at wireless network frequency bands. *IEEE Transactions on Antennas and Propagation, 62*(6), 3330–3337.
20. Gay-Fernandez, J. A., & Cuinas, I. (2013). Peer to peer wireless propagation measurements and path-loss modeling in vegetated environments. *IEEE Transactions on Antennas and Propagation, 61*(6), 3302–3311.
21. Gay-Fernández & J. A. (2011). Radio-electric validation of an electronic cowbell based on ZigBee technology. *IEEE Antennas and Propagation Magazine, 53*(4), 40–44.
22. Saunders, S. R., & Aragón-Zavala, A. (2007). *Antennas and propagation for wireless communication systems* (2nd ed., pp. 89–102). Delhi: Pashupai Printing.
23. He, R., & Zhong, Z. (2012). Analysis of the relation between Fresnel zone and path loss exponent based on two-ray model. *IEEE Antennas and Wireless Propagation Letters, 11*, 208–211.
24. Jarndal, A., & Alnajjar, K. (2018). MM-wave wideband propagation model for wireless communications in built-up environments. *Physical communication, 28*, 97–107.
25. Zang, J., & Wang, X. (2017). Measurements and modeling of path loss over irregular terrain for near-ground and short-range communications. *Progress in Electromagnetics Research M, 57*, 55–62.
26. Akyildiz, I. F., & Vuran, M. C. (2010). *Wireless sensor networks* (pp. 123–156). Wiley. ISBN-13: 978-0470036013.
27. Sawant, R. P. & Liang, Q. (2007). Experimental path loss models for wireless sensor networks. In *MILCOM 2007-IEEE Military Communications Conference*, pp. 1–7.
28. Olasupo, T., & Shaikh, S. (2015). Effects of terrain variations in wireless sensor network deployments. In *IEEE International RF and Microwave Conference (RFM)*, pp. 83–88.
29. Cassel, M., & Dépret, T. (2017). Assessment of a new solution for tracking pebbles in rivers based on active RFID. *Earth Surface Processes and Landforms, 42*(13), 1938–1951.
30. Papini, M., & Ivanov, V. I. (2017). Monitoring bedload sediment transport in a pre-alpine river: An experimental method. *Rendiconti Online Societa Geologica Italiana, 43*, 57–63.
31. Malon, K., Skokowski, P., & Lopatka, J. (2018). Optimization of wireless sensor network deployment for electromagnetic situation monitoring. *International Journal of Microwave and Wireless Technologies, 10*(7), 746–753.
32. Van Khoa, V., & Takayama, S. (2018). Wireless sensor network in landslide monitoring system with remote data management. *Measurement, 118*, 214–229.
33. Balaji, S., & Anitha, M. (2020). Energy efficient target coverage for a wireless sensor network. *Measurement, 165*, 108167.
34. Usman, M., & Gebremariam, A. A. (2015). A software-defined device-to-device communication architecture for public safety applications in 5G networks. *IEEE Access, 3*, 1649–1654.
35. Mahmoud, H. H., & ElAttar, H. M. (2017). Optimal operational parameters for 5G energy harvesting cognitive wireless sensor networks. *IETE Technical Review, 34*(sup1), 62–72.
36. Ahmadien, O., & Ates, H. F. (2020). Predicting path loss distribution of an area from satellite images using deep learning. *IEEE Access, 8*, 64982–64991.
37. Thrane, J., & Zibar, D. (2020). Model-aided deep learning method for path loss prediction in mobile communication systems at 2.6 GHz. *IEEE Access, 8*, 7925–7936.
38. Calik, N., & Belen, M. A. (2020). Deep learning base modified MLP model for precise scattering parameter prediction of capacitive feed antenna. *International Journal of Numerical Modelling: Electronic Networks, Devices and Fields, 33*(2), e2682.
39. Donkers, T., & Loepp, B. (2017). Sequential user-based recurrent neural network recommendations. In *Proceedings of the eleventh ACM conference on recommender systems*, pp. 152–160.
40. Ta, V. D., & Liu, C. M. (2020). Portfolio optimization-based stock prediction using long-short term memory network in quantitative trading. *Applied Sciences, 10*(2), 437.
41. Basyigit, I. B., Genc, A., Dogan, H., Senel, F. A., & Helhel, S. (2021). Deep learning for both broadband prediction of the radiated emission from heatsinks and heatsink optimization. *Engineering Science and Technology, an International Journal, 24*(3), 706–714.
42. Metlek, S., Kayaalp, K., Basyigit, I. B., Genc, A., & Dogan, H. (2021). The dielectric properties prediction of the vegetation depending on the moisture content using the deep neural network model. *International Journal of RF and Microwave Computer-Aided Engineering, 31*(1), e22496.
43. Roy, K., & Mandal, K. K. (2019). Ant-Lion Optimizer algorithm and recurrent neural network for energy management of micro grid connected system. *Energy, 167*, 402–416.
44. Bistron, M., & Piotrowski, Z. (2021). Artificial intelligence applications in military systems and their influence on sense of security of citizens. *Electronics, 10*(7), 871.
45. Negassi, M., & Suarez-Ibarrola, R. (2020). Application of artificial neural networks for automated analysis of cystoscopic images: A review of the current status and future prospects. *World Journal of Urology, 38*(10), 2349–2358.
46. Tran-Ngoc, H., & Khatir, S. (2021). Efficient Artificial neural networks based on a hybrid metaheuristic optimization algorithm for damage detection in laminated composite structures. *Composite Structures, 262*(113339), 1–16.
47. Alamia, A., & Gauducheau, V. (2020). Comparing feedforward and recurrent neural network architectures with human behavior in artificial grammar learning. *Scientific Reports, 10*(1), 1–15.
48 Bai, Y., & Xie, J. (2021). Regression modeling for enterprise electricity consumption: a comparison of recurrent neural network and its variants. *International Journal of Electrical Power & Energy Systems, 126*, 106612.
49. Hochreiter, S., & Schmidhuber, J. (1997). Long short-term memory. *Neural Computation, 9*(8), 1735–1780.

**Publisher's Note** Springer Nature remains neutral with regard to jurisdictional claims in published maps and institutional affiliations.

Springer Nature or its licensor (e.g. a society or other partner) holds exclusive rights to this article under a publishing agreement with the author(s) or other rightsholder(s); author self-archiving of the accepted manuscript version of this article is solely governed by the terms of such publishing agreement and applicable law.

**Kiyas Kayaalp** completed his bachelor's degree in Computer Engineering and master's degree in Electronic-Computer Education and doctorate in Physics at Süleyman Demirel University. He has working at the Isparta University of Applied Sciences. He has 3 books in the field of deep learning and software development. His research interest includes the methodologies of computer vision, including machine learning algorithms.

**Sedat Metlek** has two bachelor's degrees, namely "computer engineering" and "computer and control" education. He has a master's degree in electronic-computer education and a doctorate in electronic-communication engineering. At Burdur Mehmet Akif Ersoy University, he continues to research. He has many projects and articles in the field of deep learning and image processing. He also advises many companies in the sector on technical issues. He has a lot of books and book sections in the field of deep learning and software development.

**Abdullah Genc** received his B.Sc. degree in Electrical and Electronics Engineering from Istanbul University in 2008, M.Sc. degree in Mechanical Engineering from Rice University, in Houston, USA, in 2011, and Ph.D. degree in Electronics and Communication Engineering from Süleyman Demirel University in Isparta, in 2017. He has been working as an Assoc. Prof. in the department of Mechatronic engineering in Isparta University of Applied Sciences. His fields of interest include antennas and propagation, passive microwave components, and microwave circuit design.

**Habib Dogan** , received his B.Sc. and M.Sc. degrees in Electronics Engineering from the Erciyes University in Kayseri in 1994 and 2000, respectively, and Ph.D. degree in Electronics and Communication Engineering from Süleyman Demirel University in Isparta, in 2018. He has worked as an instructor in Harran University between 1995 and 2011. He has been working as an Assoc. Prof. in Burdur Mehmet Akif Ersoy University, Gölhisar High School of Applied Sciences. His current research interests are electromagnetic waves, electromagnetic propagation, microwave and RFID applications.

**İbrahim Bahadir Basyigit** , received his B.Sc. degree in Electrical and Electronics Engineering from the Sakarya University in 2005, M.Sc. degree in Electrical and Electronics Engineering from the Akdeniz University, in Antalya, in 2011 and Ph.D. degree in Electronics and Communication Engineering from Süleyman Demirel University in Isparta, in 2016. He has been working as an Assoc. Prof. in Distance Learning Vocational School in Isparta University of Applied Sciences. His current research interests are among of electromagnetic compatibility, electromagnetic waves, electromagnetic propagation, and cellular networks.